IEEE Access
Multidisciplinary | Rapid Review | Open Access Journal

Received June 18, 2021, accepted July 23, 2021, date of publication August 3, 2021, date of current version August 13, 2021.

Digital Object Identifier 10.1109/ACCESS.2021.3102083

Stability Limits for the Velocity Orientation Autopilot of Rolling Missiles

SHAOYONG HU[1,2], JIANG WANG[1,2], YUCHEN WANG[1,2], AND SONG TIAN[3]

[1]School of Aerospace Engineering, Beijing Institute of Technology, Beijing 100081, China
[2]Beijing Key Laboratory of UAV Autonomous Control, Beijing Institute of Technology, Beijing 100081, China
[3]Beijing System Design Institute of Electro-Mechanic Engineering, Beijing 100039, China

Corresponding author: Yuchen Wang (wyccbit@163.com)

This work was supported by the Natural Science Foundation of China under Grant 61172182 and Grant U1613225.

ABSTRACT In this paper, we derive the sufficient and necessary stability conditions for rolling missiles with velocity orientation autopilot. For the mathematical derivation, linear time-invariant mathematical models are established. Structures of the velocity orientation autopilot for nonrolling and rolling missiles are introduced. In addition, the effects of the autopilot structure and parameters on stability are discussed. Furthermore, methods associated with actuator dynamics, static stability and decoupling are presented to improve the stability of rolling missiles. Numerical simulations are conducted to verify the accuracy of the discussion. It is demonstrated that the stability conditions can guide rolling missile velocity orientation autopilot design for the stabilization of the flight of rolling missiles.

INDEX TERMS Rolling missile, coning motion, velocity orientation autopilot, dynamic stability, stability improving methods.

NOTATION

Symbol	Definition (Unit)
J_z	lateral moment of inertial($kg \bullet m^2$)
J_x	longitudinal moment of inertial($kg \bullet m^2$)
q	dynamic pressure(N/m^2)
s_{ref}	reference area(m^2)
l	reference length(m)
d	airframe diameter(m)
m	mass of missile(kg)
V	scalar velocity(m/s)
P	thrust force(N)
θ_c	flight-path angle command(rad)
ψ_{Vc}	heading angle command(rad)
θ	flight-path angle(rad)
ψ_V	heading angle(rad)
k_z	gain of velocity angle position feedback($-$)
k_ω	gain of attitude angular rate feedback($-$)
e_y, e_z	angle error(rad)
δ_{yc}, δ_{zc}	deflection command(rad)
ϑ	pitch angle(rad)
γ	roll angle(rad)
M_z^α	derivative of static moment coefficient($-$)
M_z^β	derivative of Magnus moment coefficient($-$)
$M_z^{\omega_z}$	derivative of damping moment coefficient($-$)
$M_z^{\delta_z}$	derivative of control moment coefficient($-$)
c_y^α	derivative of lift coefficient($-$)
c_y^β	derivative of Magnus force coefficient($-$)
γ_d	total deviation angle of control system(rad)
γ_c	steady-state deviation angle(rad)
τ	time delay of command transmission(s)
k_r	equivalent dynamic gain($-$)
k_s	gain of actuator($-$)
T_s	time constant of actuator(s)
μ_s	damping ratio of actuator($-$)
δ	complex deflection angle($-$)
α_C	complex angle of attack($-$)
δ_y, δ_z	deflection in nonrolling coordinate system (rad)
ψ	yaw angle(rad)

The associate editor coordinating the review of this manuscript and approving it for publication was Rosario Pecora.

I. INTRODUCTION

Velocity orientation autopilot is a typical autopilot that can improve the damping characteristics and increase the stability and interference rejection capability of missiles.

Due to its simple and easy-to-implement structure, many guided weapons have utilized this type of autopilot for extended range and realization of body pursuit guidance. In manual control systems, velocity orientation autopilot is often used to control the velocity orientation of missiles to be straight [1]. Usually, missiles with velocity orientation autopilot are employed for attacking static and low-speed targets, and some gliding missiles need to use a velocity orientation autopilot to achieve speed tracking during the gliding phase under the velocity pursuit guidance law [2]–[4]. Most of the missiles are designed to roll during flight to decrease hitting dispersion. The stability conditions and design methods of missiles with velocity orientation autopilot are discussed based on the assumption that the two perpendicular control channels (i.e., pitching and yawing) of the missiles can be separated [5]–[7]. The results are effective in nonrolling cases. However, for rolling missiles, the rolling of the airframe induces cross-coupling effects, which may worsen the stability of the velocity orientation autopilot. Therefore, the stability conditions based on the separation assumption are no longer valid in rolling cases.

For rolling missiles, most studies on the dynamic stability of the coning motion have been devoted to uncontrolled missiles [8]–[10]. In a paper by Mracek *et al.*, it was pointed out that rolling of the airframe affects both the response and the stability of the autopilot [11]. The influence of cross-coupling effects on the stability of missiles has been widely investigated [12]–[17]. Garnell found that a phase lag in the actuators appeared near the rolling frequency of missiles. The frequency method was utilized in further analysis to reveal the impacts on the autopilot's stability conditions [5]. For rolling missiles with a rate loop and an attitude autopilot, Yan *et al.* proposed suitable design conditions that can stabilize the coning motion to guide autopilot design [18], [19]. Similar studies on rolling missiles with acceleration autopilot were performed by Li *et al.*, and sufficient and necessary conditions were proposed [20]. However,limited studies have pay attention on the stability conditions of the coning motion of rolling missiles with velocity orientation autopilot which is commonly used. Therefore, it is crucial to analyze the stability conditions of autopilot for these cases and to find the autopilot design parameter boundaries to guarantee flight stability.

Motivated by the previously mentioned works, this paper proposes the stability criterion of the velocity orientation autopilot of a rolling missile. The main contributions and innovations are summarized as follows:

- The sufficient and necessary condition for the stability of a spinning missile with the velocity orientation autopilot is proposed analytically using a complex summation method.
- Case studies and comparison between a rolling frame and nonrolling frame show that the rolling frame narrows the stable region.
- Considering the existence of coupling, this paper analyzes the dynamic of an actuator and the influence of missile static parameters and further proposes a practical leading angel decoupling method.

The remainder of this paper is arranged as follows: In Section II, the mathematical model of the velocity orientation autopilot is formulated. In Section III, the structure of the velocity orientation autopilot in the pitching channel is illustrated, stability conditions are obtained, and numerical simulations are conducted to verify the validity of the conditions. In Section IV, methods associated with the actuator dynamics, static stability and decoupling are introduced. The simulation results demonstrate the effectiveness of the decoupling method and robustness of the designed autopilot. Conclusions are presented in Section V.

II. MATHEMATICAL MODEL

A. COORDINATE SYSTEMS

To describe the airframe motion equations, we introduce four relevant coordinate systems: datum coordinate systems, body coordinate systems, nonspinning body coordinate systems, and velocity coordinate systems. The definitions of these coordinate systems are given as follows [21]:

The datum coordinate system $Ox_0y_0z_0$ is assumed to be an inertial coordinate frame and the body coordinate system $Ox_by_bz_b$ is a spinning frame and fixes the missile. As shown in Fig. 1, the nonspinning body coordinate system $Ox_{nb}y_{nb}z_{nb}$ can be obtained by sequentially rotating $Ox_0y_0z_0$ by angles ϑ and ψ. And $Ox_by_bz_b$ can be obtained by rotating $Ox_{nb}y_{nb}z_{nb}$ by the angle γ about x-axis. The matrix for transforming $Ox_0y_0z_0$ to $Ox_{nb}y_{nb}z_{nb}$ is

$$\begin{aligned} R_0^{nb} &= R(\psi)R(\vartheta) \\ &= \begin{bmatrix} \cos\psi & 0 & -\sin\psi \\ 0 & 1 & 0 \\ \sin\psi & 0 & \cos\psi \end{bmatrix} \begin{bmatrix} \cos\vartheta & \sin\vartheta & 0 \\ -\sin\vartheta & \cos\vartheta & 0 \\ 0 & 0 & 1 \end{bmatrix} \\ &= \begin{bmatrix} \cos\psi\cos\vartheta & \cos\psi\sin\vartheta & -\sin\psi \\ -\sin\vartheta & \cos\vartheta & 0 \\ \sin\psi\cos\vartheta & \sin\psi\sin\vartheta & \cos\psi \end{bmatrix} \end{aligned} \tag{1}$$

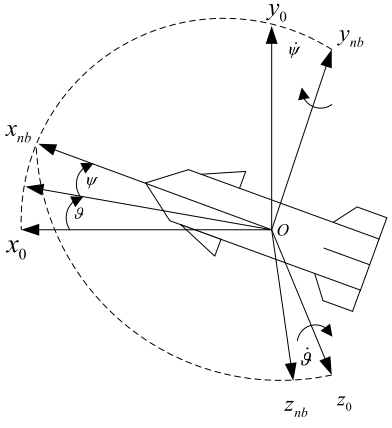

FIGURE 1. Relative angle between the datum coordinate system and nonspinning body coordinate system.

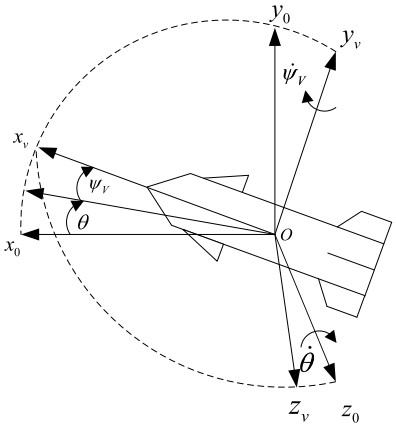

FIGURE 2. Relative angle between the datum coordinate system and the velocity coordinate system.

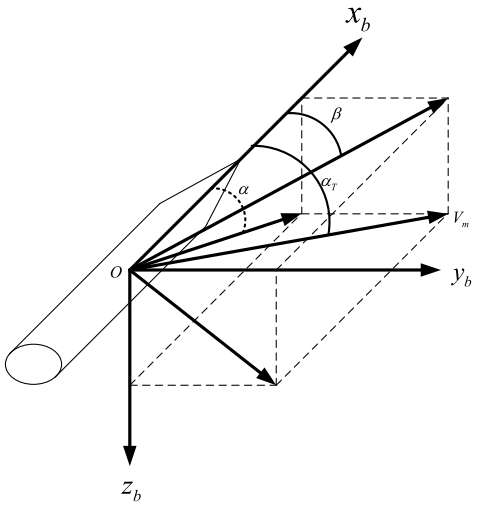

FIGURE 3. Relative angle between the body coordinate system and the velocity vector.

For the velocity coordinate system $Ox_vy_vz_v$, Ox_v aligns with the velocity vector, as shown in Fig. 2. $Ox_vy_vz_v$ can be obtained by rotating $Ox_0y_0z_0$ by angles θ and ψ_V in the same way as in the definition of the nonspinning body coordinate system. The matrix for transforming $Ox_0y_0z_0$ to $Ox_vy_vz_v$ is

$$\begin{aligned} R_0^{\text{vel}} &= R(\psi_V)R(\theta) \\ &= \begin{bmatrix} \cos\psi_V & 0 & -\sin\psi_V \\ 0 & 1 & 0 \\ \sin\psi_V & 0 & \cos\psi_V \end{bmatrix} \begin{bmatrix} \cos\theta & \sin\theta & 0 \\ -\sin\theta & \cos\theta & 0 \\ 0 & 0 & 1 \end{bmatrix} \\ &= \begin{bmatrix} \cos\psi_V\cos\theta & \cos\psi_V\sin\theta & -\sin\psi_V \\ -\sin\theta & \cos\theta & 0 \\ \sin\psi_V\cos\theta & \sin\psi_V\sin\theta & \cos\psi_V \end{bmatrix} \end{aligned} \tag{2}$$

Note that $Ox_vy_vz_v$ can be transformed into $Ox_{nb}y_{nb}z_{nb}$ by rotating a particular angle around the z-axis and a particular angle around the subsequent y-axis, as depicted in Fig. 3 [22]. where α_T is the total angle of attack and α and β are the nonspinning angle of attack and nonspinning sideslip angle, respectively. The matrix for transforming $Ox_vy_vz_v$ to $Ox_{nb}y_{nb}z_{nb}$ is

$$\begin{aligned} R_{\text{vel}}^{nb} &= R(\beta)R(\alpha) \\ &= \begin{bmatrix} \cos\beta & 0 & -\sin\beta \\ 0 & 1 & 0 \\ \sin\beta & 0 & \cos\beta \end{bmatrix} \begin{bmatrix} \cos\alpha & \sin\alpha & 0 \\ -\sin\alpha & \cos\alpha & 0 \\ 0 & 0 & 1 \end{bmatrix} \\ &= \begin{bmatrix} \cos\beta\cos\alpha & \cos\beta\sin\alpha & -\sin\beta \\ -\sin\alpha & \cos\alpha & 0 \\ \sin\beta\cos\alpha & \sin\beta\sin\alpha & \cos\beta \end{bmatrix} \end{aligned} \tag{3}$$

B. AERODYNAMICS OF THE MISSILE BODY

As previously stated, the missile involved in this paper has an axisymmetric aerodynamic configuration. Without a loss of generality, the derivative coefficients of the yawing channel are replaced by that of the pitching channel to simplify the expression of the airframe motion equations. According to Garnell [2], assuming that the velocity and rolling rate remain constant over a short interval in the flight and neglecting some small forces and moments, the dynamic equations of rolling missiles can be written in the nonspinning body frame as:

$$\begin{cases} \dfrac{d^2\vartheta}{dt^2} = \dfrac{M_z^\alpha}{J_z}\alpha + \dfrac{M_z^\beta}{J_z}\beta + \dfrac{J_x}{J_z}\omega_x\dfrac{d\psi}{dt} + \dfrac{M_z^{\omega_z}}{J_z}\dfrac{d\vartheta}{dt} + \dfrac{M_z^{\delta_z}}{J_z}\delta_z \\ \dfrac{d^2\psi}{dt^2} = \dfrac{M_z^\alpha}{J_z}\beta + \dfrac{M_z^\beta}{J_z}\alpha - \dfrac{J_x}{J_z}\omega_x\dfrac{d\vartheta}{dt} + \dfrac{M_z^{\omega_z}}{J_z}\dfrac{d\psi}{dt} + \dfrac{M_z^{\delta_z}}{J_z}\delta_y \\ \dfrac{d\theta}{dt} = \dfrac{P+Y^\alpha}{mV}\alpha + \dfrac{Y^\beta}{mV}\beta \\ \dfrac{d\psi_V}{dt} = \dfrac{P+Y^\alpha}{mV}\beta - \dfrac{Y^\beta}{mV}\alpha \\ \alpha = \vartheta - \theta \\ \beta = \psi - \psi_V \end{cases} \tag{4}$$

With the linearization of the coefficients of the aerodynamic forces and moments, a more concise expression of the airframe motion equation can be obtained as

$$\begin{cases} \ddot{\vartheta} = -a_L\alpha - a_M\beta + a_G\dot{\psi} - a_\omega\dot{\vartheta} - a_\delta\delta_z \\ \ddot{\psi} = -a_L\beta + a_M\alpha - a_G\dot{\vartheta} - a_\omega\dot{\psi} - a_\delta\delta_y \\ \dot{\theta} = b_L\alpha + b_M\beta \\ \dot{\psi}_V = b_L\beta - b_M\alpha \\ \alpha = \vartheta - \theta \\ \beta = \psi - \psi_V \end{cases} \tag{5}$$

where $a_L = -\frac{M_z^\alpha}{J_z} = -m_z^\alpha\frac{qs_{ref}l}{J_z}$, $a_M = -\frac{M_z^\beta}{J_z} = -m_z^\beta\frac{qs_{ref}l}{J_z}\left(\frac{\omega d}{V}\right)$, $a_G = \frac{J_x}{J_z}\omega$, $a_\omega = -\frac{M_z^{\omega_z}}{J_z} = -m_z^{\omega_z}\frac{qs_{ref}l}{J_z}\left(\frac{l}{V}\right)$. $a_\delta = -\frac{M_z^{\delta_z}}{J_z} = -m_z^{\delta_z}\frac{qs_{ref}l}{J_z}$, $b_L = \frac{P+Y^\alpha}{mV} = c_y^\alpha\frac{qs_{ref}}{mV} + \frac{P}{mV}$, $b_M = \frac{Y^\beta}{mV} = -c_y^\beta\frac{qs_{ref}}{mV}\left(\frac{\omega d}{V}\right)$ and $\omega = \dot{\gamma}$.

With the definition of complex variables $\alpha_C = \beta + i\alpha$ and $\delta = \delta_y + i\delta_z$, the linearized angular motion of rolling missiles can be obtained as

$$\ddot{\alpha}_C = \begin{bmatrix} -(a_L + a_G b_M + a_\omega b_L) \\ -i(a_M - a_G b_L + a_\omega b_M) \end{bmatrix} \alpha_C - (a_\omega - i a_G)\dot{\alpha}_C - (b_L + i b_M)\dot{\alpha}_C - a_\delta \delta \quad (6)$$

This equation defines a complex differential equation between complex canard deflection and complex angles of attack.

C. DYNAMICS OF THE ACTUATORS

In this paper, the dynamics of the actuators that we utilized are modeled as a second-order transfer function.

$$\frac{\delta_a}{\delta_c} = \frac{k_s}{T_s^2 s^2 + 2\mu_s T_s s + 1} \quad (7)$$

where T_s is the time constant of the actuators, μ_s is the damping ratio, and k_s is the gain. The time constant is limited by the hardware and the costs.

The airframe of a nonspinning missile does not rotate continuously. Both the inertia sensors and the servo work in the same reference coordinate system (body coordinate system). Therefore, there is no need to consider the coordinate transformation between the feedback information and the command when analyzing the autopilot. The desired gain can be obtained by conventional root locus or frequency approaches.

Generally, for a nonrolling missile, the actuators and autopilot work in the same reference coordinate system (body coordinate system). However, when the missile is rolling, the actuators work in the body coordinate system, while the autopilot functions in the nonrolling body coordinate system. Because of the difference in the reference coordinate systems, control cross-coupling between two channels is induced by the rolling of the airframe. The projection of the responses of the actuators from the body coordinates to the nonrolling body coordinates shows that the control cross-coupling leads to a deviation in the equivalent control forces and a decrease in the efficiency of the actuators. These two effects can be shown as the steady-state deviation angle and equivalent dynamic gain.

The steady-state deviation angle of the actuators in the nonrolling body coordinates of a rolling missile can be expressed as follows:

$$\gamma_c = \arccos \frac{1 - T_s^2\omega^2}{\sqrt{\left(1 - T_s^2\omega^2\right)^2 + (2\mu_s T_s \omega)^2}} \quad (8)$$

The equivalent dynamic gain of the actuators in the nonrolling body coordinates of a rolling missile can be expressed as

$$k_r = \frac{1}{\sqrt{\left(1 - T_s^2\omega^2\right)^2 + (2\mu_s T_s \omega)^2}} \quad (9)$$

In addition, the existence of command transmission delay τ, which can be easily identified by experiments, can lead to a deviation angle equal to $\tau\omega$. For the actuators of a self-rolling missile, the total deviation angle γ_d equals $(\gamma_c + \tau\omega)$, as illustrated in Fig. 4.

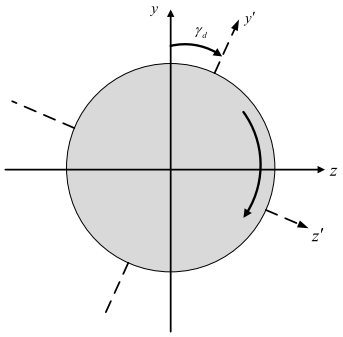

FIGURE 4. Total deviation angle.

As the same actuators are employed in the two control channels, the outputs of the actuators can be obtained as

$$\begin{bmatrix} \delta_z \\ \delta_y \end{bmatrix} = k_s k_r \begin{bmatrix} \cos\gamma_d & \sin\gamma_d \\ -\sin\gamma_d & \cos\gamma_d \end{bmatrix} \begin{bmatrix} \delta_{zc} \\ \delta_{yc} \end{bmatrix} \quad (10)$$

where δ_{zc} *and* δ_{yc} are the commands of the actuators in pitching and yawing, respectively.

With the definition of $\delta_c = \delta_{yc} + i\delta_{zc}$ as the complex command of the actuator, expression (10) can be rewritten as

$$\begin{aligned} \delta &= k_s k_r \left(-\delta_{zc}\sin\gamma_d + \delta_{yc}\cos\gamma_d\right) \\ &\quad + i k_s k_r \left(\delta_{zc}\cos\gamma_d + \delta_{yc}\sin\gamma_d\right) \\ &= k_s k_r \left(\cos\gamma_d + i\sin\gamma_d\right)\delta_c \end{aligned} \quad (11)$$

III. STABILITY ANALYSIS OF MISSILES WITH VELOCITY ORIENTATION AUTOPILOT

A. FOR NONROLLING MISSILES

A typical velocity orientation autopilot mainly consists of attitude angular rate feedback and velocity angle position feedback. The block diagram of the velocity orientation autopilot in pitching based on the established mathematical model is presented in Fig. 5.

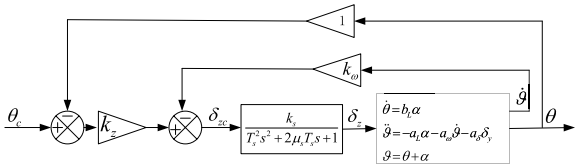

FIGURE 5. Velocity orientation autopilot for nonrolling missiles.

From Fig. 5, the expressions of the missile motions can be obtained in the form of a transfer function

$$\frac{\dot{\vartheta}(s)}{\delta_z(s)} = \frac{-a_\delta(s + b_L)}{s^2 + (b_L + a_\omega)s + (a_L + b_L a_\omega)} \quad (12)$$

and

$$\frac{\theta(s)}{\dot{\vartheta}(s)} = \frac{b_L}{s\,(s+b_L)} \tag{13}$$

From Fig. 5, the structure of the velocity orientation autopilot can be separated into an inner loop, i.e., an attitude angular rate feedback loop, and an outer loop, i.e., a velocity angle position feedback loop, and the stability condition of the total closed loop system can be converted to the corresponding subsystem.

Initially, disregarding the dynamic process in this system, i.e., considering only the steady state [20], the closed-loop transfer function of the velocity orientation autopilot can be obtained as

$$\begin{aligned} \frac{\theta(s)}{\theta_c(s)} &\triangleq \frac{N_1}{M_1} \\ N_1 &= -b_L k_z k_s a_s \\ M_1 &= s^3 + \begin{pmatrix} b_L + a_\omega \\ -k_s k_\omega a_\delta \end{pmatrix} s^2 + \begin{pmatrix} a_L + a_\omega b_L \\ -b_L k_\omega k_s a_\delta \end{pmatrix} s \\ &\quad - b_L k_z k_s a_\delta \end{aligned} \tag{14}$$

Based on the Routh-Hurwitz criterion, the stability conditions yield

$$\begin{cases} b_L + a_\omega - k_s k_\omega a_\delta > 0 \\ a_L + a_\omega b_L - b_L k_s k_\omega a_\delta > 0 \\ -b_L k_z k_s a_\delta > 0 \\ \begin{pmatrix} (b_L + a_\omega - k_s k_\omega a_\delta)\,(a_L + a_\omega b_L - b_L k_s k_\omega a_\delta) \\ +b_L k_z k_s a_\delta \end{pmatrix} > 0 \end{cases} \tag{15}$$

According to the definition, the coefficients b_L and a_ω are positive and a_δ is negative for missiles with canard configurations. As a result, the first and third inequalities in Eq. (15) always hold true. The stability conditions can be simplified as

$$\begin{cases} a_L + a_\omega b_L - b_L k_s k_\omega a_\delta > 0 \\ \begin{pmatrix} (b_L + a_\omega - k_s k_\omega a_\delta)\,(a_L + a_\omega b_L - b_L k_s k_\omega a_\delta) \\ +b_L k_z k_s a_\delta \end{pmatrix} > 0 \end{cases} \tag{16}$$

Therefore, the stability conditions of the velocity orientation autopilot is general. The stability conditions under different circumstances is discussed as follows:

1) CASE WITH ONLY THE INNER LOOP

In this case, we disregard the gain of the outer loop (velocity angle position feedback loop) of the autopilot, i.e., the gain of the outer loop is 0. Therefore, the stability conditions for the inner loop (attitude angular rate feedback loop) can be formulated as

$$\begin{cases} a_L + a_\omega b_L - b_L k_s k_\omega a_\delta > 0 \\ (b_L + a_\omega - k_s k_\omega a_\delta)\,(a_L + a_\omega b_L - b_L k_s k_\omega a_\delta) > 0 \end{cases} \tag{17}$$

that is,

$$k_\omega > -\left(a_L + a_\omega b_L\right) / -b_L k_s k_\omega a_\delta \tag{18}$$

For a static stable missile, $a_L > 0$, and the lower limit of the gain of the rate feedback is $k_\omega > 0$. However, for static unstable missiles, $a_L < 0$. Considering the case of $|a_L| > a_\omega b_L$, the lower limit of the gain of the rate feedback is $k_\omega > -\left(a_L + a_\omega b_L\right) / \left(-b_L k_s k_\omega a_\delta\right)$, which means that a k_ω larger than that of a static stable missile is needed to stabilize a static unstable missile. Therefore, the static stability of the missile has many effects on the stability of the velocity orientation autopilot.

2) CASE WITH ONLY THE OUTER LOOP

Disregarding the inner loop, i.e., k_ω is 0, we can obtain the conditions for the outer loop.

$$\begin{cases} a_L + a_\omega b_L > 0 \\ a_L + a_\omega b_L > -b_L k_z k_s a_\delta / \left(b_L + a_\omega\right) \end{cases} \tag{19}$$

The existence of the outer loop tends to degrade the stability of the autopilot and is unable to stabilize a static unstable missile solely by the outer loop. Hence, the inner loop is necessary to stabilize a velocity orientation autopilot regardless of whether the missile is statically stable.

B. FOR SELF-ROLLING MISSILES

In this subsection, velocity orientation autopilot is applied in both the pitching channel and the yawing channel. The rolling of missiles induces cross-coupling and degrades the stability of the autopilot and can even cause autopilot instability. Therefore, to ensure the stability of the designed autopilot, it is better to consider the two control channels as an integral control system and to analyze the stability conditions. The block diagram of the integral control system is shown in Fig. 6.

According to the structure of the autopilot shown in Fig. 6, the error signals in the pitching and yawing channels can be expressed as

$$\begin{bmatrix} e_z \\ e_y \end{bmatrix} = \begin{bmatrix} k_z\theta_c - k_z\theta - k_\omega\dot{\vartheta} \\ k_z\left(-\psi_{Vc}\right) + k_z\psi_V + k_\omega\dot{\psi} \end{bmatrix} \tag{20}$$

For missiles with canard configurations, to produce positive α, the deflection of the control surface in pitching should be positive. A negative deflection of the control surface in yawing is needed to produce a negative β. Hence, the commands of the control surfaces can be described as

$$\begin{aligned} \begin{bmatrix} \delta_{zc} \\ \delta_{yc} \end{bmatrix} &= \begin{bmatrix} 1 & 0 \\ 0 & -1 \end{bmatrix} \begin{bmatrix} e_z \\ e_y \end{bmatrix} \\ &= \begin{bmatrix} k_z\theta_c - k_z\theta - k_\omega\dot{\vartheta} \\ -k_z\left(-\psi_{Vc}\right) - k_z\psi_V - k_\omega\dot{\psi} \end{bmatrix} \end{aligned} \tag{21}$$

Remark 1: To further illustrate the effect of the rolling frame, similar to the last section, the response delay of the actuator is neglected.

For a linear time-invariant system, the stability is free from the impact of input signals. As a result, the input signals θ_c and ψ_{Vc} can be set to zero in the stability analysis. With the

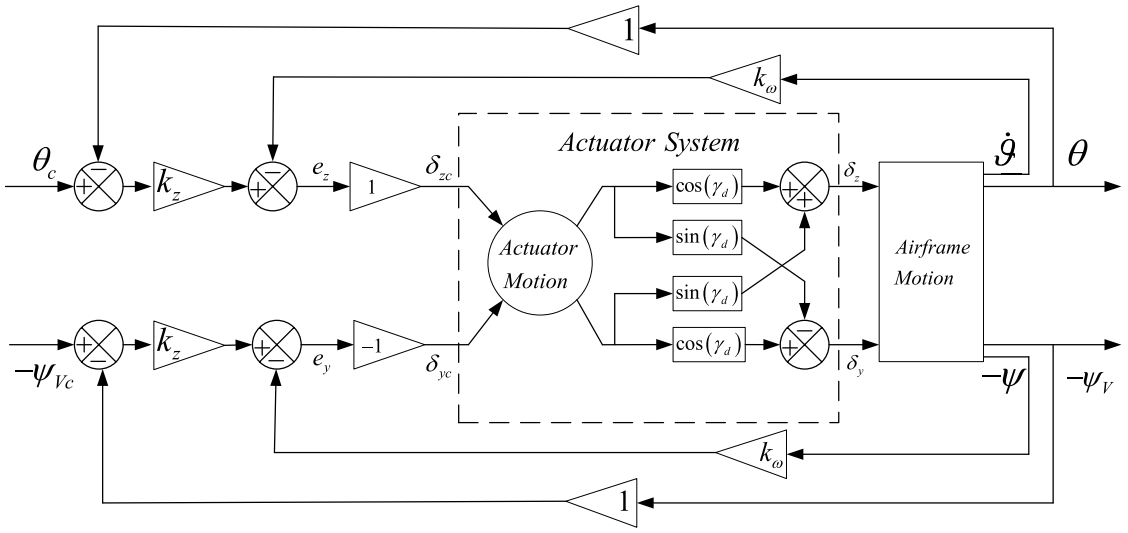

FIGURE 6. Structure of the velocity orientation autopilot for a rolling missile.

definition of $\phi = \psi_V + i\theta$, expression (21) can be simplified and rewritten as

$$\delta_c = \delta_{yc} + i\delta_{zc} = -k_z\phi - k_\omega\left(b_L + ib_M\right)\alpha_C - k_\omega\dot{\alpha}_C \quad (22)$$

Substituting (22) into (11), the following equation can be obtained:

$$\delta = k_s k_r\left(\cos\gamma_d + i\sin\gamma_d\right)\begin{pmatrix} -k_z\phi - k_\omega\left(b_L + ib_M\right)\alpha_C \\ -k_\omega\dot{\alpha}_C \end{pmatrix} \quad (23)$$

By substituting (23) into (6), the following equation can be obtained:

$$\begin{pmatrix} \ddot{\alpha}_C + \left(M_1 + iN_1\right)\dot{\alpha}_C + \left(M_2 + iN_2\right)\alpha_C \\ -a_\delta k_s k_r\left(\cos\gamma_d + i\sin\gamma_d\right)k_z\phi \end{pmatrix} = 0 \quad (24)$$

where

$$\begin{aligned} &M_1 + iN_1 \\ &= a_\omega + b_L - a_\delta k_s k_r k_\omega\cos\gamma_d + i\begin{pmatrix} b_M - a_G \\ -a_\delta k_s k_r k_\omega\sin\gamma_d \end{pmatrix} \end{aligned} \quad (25)$$

$$\begin{aligned} &M_2 + iN_2 \\ &= \left(a_L + a_G b_M + a_\omega b_L\right) - a_\delta k_s k_r k_\omega\left(b_L\cos\gamma_d - b_M\sin\gamma_d\right) \\ &\quad + i\begin{bmatrix} \left(a_M - a_G b_L + a_\omega b_M\right) \\ -a_\delta k_s k_r k_\omega\left(b_M\cos\gamma_d + b_L\sin\gamma_d\right) \end{bmatrix} \end{aligned} \quad (26)$$

$x = \begin{bmatrix}\phi & \alpha_C & \dot{\alpha}_C\end{bmatrix}^T$ is defined as the state vector, and the state equation of the velocity orientation autopilot can be presented as

$$\dot{x} = \begin{bmatrix} 0 & b_L + ib_M & 0 \\ 0 & 0 & 1 \\ x_{31} & -\left(M_2 + iN_2\right) & -\left(M_1 + iN_1\right) \end{bmatrix} x \quad (27)$$

where $x_{31} = a_\delta k_s k_r\left(\cos\gamma_d + i\sin\gamma_d\right)k_z$.

The characteristic equation can be written as:

$$\lambda^3 + \left(M_1 + iN_1\right)\lambda^2 + \left(M_2 + iN_2\right)\lambda + \left(M_3 + iN_3\right) = 0 \quad (28)$$

where

$$\begin{aligned} M_3 + iN_3 &= -a_\delta k_s k_r\left(\cos\gamma_d + i\sin\gamma_d\right)k_z\left(b_L + ib_M\right) \\ &= -a_\delta k_s k_r k_z\left(b_L\cos\gamma_d - b_M\sin\gamma_d\right) \\ &\quad - ia_\delta k_s k_r k_z\left(b_M\cos\gamma_d + b_L\sin\gamma_d\right) \end{aligned} \quad (29)$$

For a system with a characteristic equation, such as Eq. (29), the stability conditions of the system can be expressed by its coefficients. The following theorem gives specific expressions.

Theorem 1: For a third-order linear characteristic equation with complex coefficients of form,

$$\lambda^3 + \left(a_1 + jb_1\right)\lambda^2 + \left(a_2 + jb_2\right)\lambda + a_3 + jb_3 = 0 \quad (30)$$

where $a_1, b_1, a_2, b_2, a_3, b_3 \in \mathbb{R}$, and the necessary and sufficient stability conditions of the system are

$$\begin{cases} a_1 > 0 \\ a_1^2 a_2 - a_1 a_3 + a_1 b_1 b_2 - b_2^2 > 0 \\ \left(a_1^2 a_2 - a_1 a_3 + a_1 b_1 b_2 - b_2^2\right)\left(a_1 a_2 a_3 - a_3^2 + a_1 b_2 b_3\right) \\ -\left(a_1^2 b_3 - a_1 a_3 b_1 + a_3 b_2\right)^2 > 0 \end{cases} \quad (31)$$

Proof can be found in [23].

Therefore, with the system characteristic equation Eq. (28), the stability conditions of the velocity orientation autopilot can be expressed as

$$\begin{cases} M_1 > 0 \\ M_1^2 M_2 - M_1 M_3 + M_1 N_1 N_2 - N_2^2 > 0 \\ P_1 P_2 - P_3^2 > 0 \end{cases} \quad (32)$$

where

$$\begin{cases} P_1 = M_1^2 M_2 - M_1 M_3 + M_1 N_1 N_2 - N_2^2 \\ P_2 = M_1 M_2 M_3 - M_3^2 + M_1 N_2 N_3 \\ P_3 = M_1^2 N_3 - M_1 M_3 N_1 + M_3 N_2 \end{cases}$$

According to the definitions of (25), (26) and (29), the stability conditions can be expressed in a specific form. The first inequality is

$$a_\omega + b_L - a_\delta k_s k_r k_\omega \cos\gamma_d > 0 \tag{33}$$

When $\gamma_d > \pi/2$, the value of $\cos\gamma_d$ is negative. Thus, the condition can be expressed as

$$k_\omega < \frac{a_\omega + b_L}{a_\delta k_s k_r \cos\gamma_d}$$

It is indicated that the gain k_ω for the inner loop has an upper limit of the total deviation angle $\gamma_d > \pi/2$. The upper limit is usually small, as the coefficient of damping moment a_ω and coefficient of lift b_L are small. When $0 < \gamma_d < \pi/2$, the first inequality is always satisfied as $\cos\gamma_d > 0$, $b_L > 0$ and $a_\omega > 0$. Hence, in general, the total deviation angle should be kept under $\pi/2$. In the next discussion, it is assumed that the total deviation angle $0 < \gamma_d < \pi/2$. The stability of the autopilot and stable region under a rolling frame are discussed as follows:

Considering only the inner loop of the autopilot, $M_3 = N_3 = 0$, and the stability conditions can be obtained as

$$\begin{cases} M_1 > 0 \\ M_1^2 M_2 + M_1 N_1 N_2 > N_2^2 \end{cases} \tag{34}$$

Based on the assumption of $0 < \gamma_d < \pi/2$, the first inequality always holds true, so the stability conditions can be rewritten as

$$M_1 M_2 + N_1 N_2 > N_2^2 / M_1 \tag{35}$$

As the Magnus force and gyroscopic moment are small, both can be neglected; so $b_M = 0$ and $a_G = 0$. The specific expression of the stability conditions of the inner loop is obtained as Eq. (36), shown at the bottom of the page.

Disregarding the effects of the actuator, which means that $k_r = 1$ and $\gamma_d = 0$, the condition can be presented as Eq. (37), shown at the bottom of the page.

Comparing this expression with Eq. (17), it is clear that the Magnus effect shrinks the stable region of the gain of the inner loop. With the effects of the actuators, the reduction in the stable region is large. All these effects derive from the rolling of the missile body, so the impact of rolling on stability should be considered in the design of an autopilot.

In the previous discussion, the influence of rolling on the stability of the autopilot are revealed. However, due to the complex expressions, it is hard for us to conduct further discussion by means of simplification. Fortunately, numerical methods can be employed to continue this work.

The parameters of the rolling missile are given in TABLE 1. Through numerical simulation, we can obtain the stable region at the rolling rate $\omega = 8\pi\ rad/s$, as shown in Fig. 7.

TABLE 1. Parameters of the rolling missile.

Parameter	Value	Parameter	Value
c_y^α	10.03	J_x/J_z	3.148×10^{-3}
c_y^β	-1.103	V	1200
m_z^α	-0.6589	k_s	10
m_z^β	5.357	μ_s	0.5
$m_z^{\omega_z}$	-1.777	T_s	0.016
$m_z^{\delta_z}$	0.0546	τ	0.015

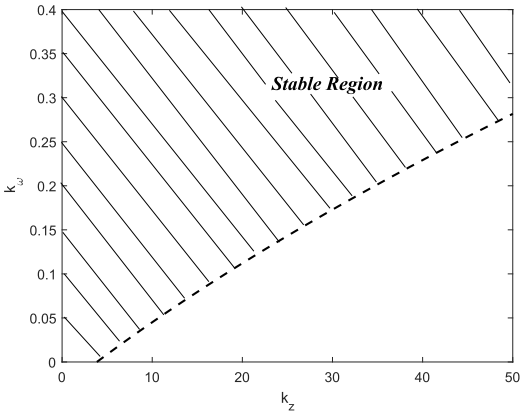

FIGURE 7. Stable region obtained from the stability conditions.

Fig. 7 illustrates the stable region of the autopilot design parameters; this region is determined with the stability conditions obtained with the proposed method. From Fig. 7, it can be seen that the stable region has only a lower limit. As k_z increases, the critical value of k_ω increases and then gradually slows, which means that the stability of the autopilot decreases with an increase in k_z and requires a larger inner loop gain to maintain stability. With an increase in k_ω, the stability of the autopilot is improved. Obviously, these conclusions match those of the nonrolling case.

To check the accuracy of the stability conditions in an intuitive way, numerical simulations are conducted based on the mathematical model in Eq. (5). With $k_z = 12.5$, the critical value of $k_\omega = 0.086$ is calculated at $\omega = 8\pi\ rad/s$.

$$\begin{aligned} &(a_\omega + b_L - a_\delta k_s k_r k_\omega \cos\gamma_d)(a_L + a_\omega b_L - a_\delta b_L k_s k_r k_\omega \cos\gamma_d) + (-a_\delta k_s k_r k_\omega \sin\gamma_d)(a_M - a_\delta b_L k_s k_r k_\omega \sin\gamma_d) \\ &\quad > (a_M + b_L(-a_\delta k_r k_s) k_\omega \sin\gamma_d)^2 / (a_\omega + b_L + (-a_\delta k_r k_s) k_\omega \cos\gamma_d) \end{aligned} \tag{36}$$

$$(a_\omega + b_L - k_s k_\omega a_\delta)(a_L + a_\omega b_L - b_L k_s k_\omega a_\delta) > (a_M)^2 / (a_\omega + b_L + (-a_\delta k_s) k_\omega) \tag{37}$$

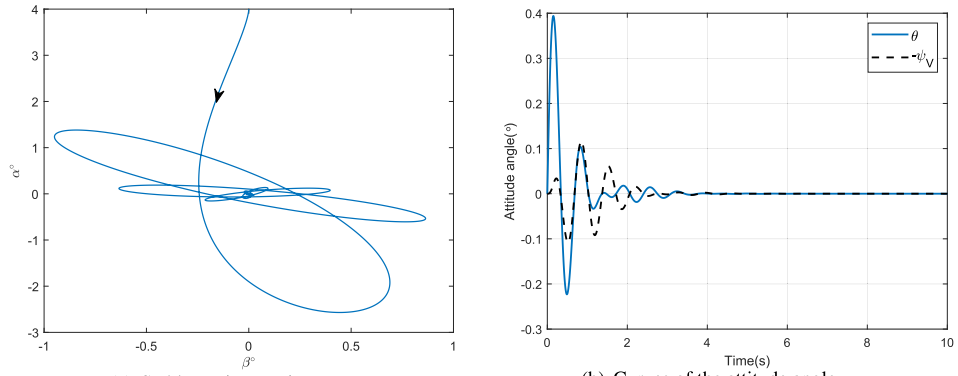

(a) Stable coning motion (b) Curves of the attitude angle

FIGURE 8. Response curves with design parameters inside the stable region ($K_Z = 12.5, k_\omega = 0.15$).

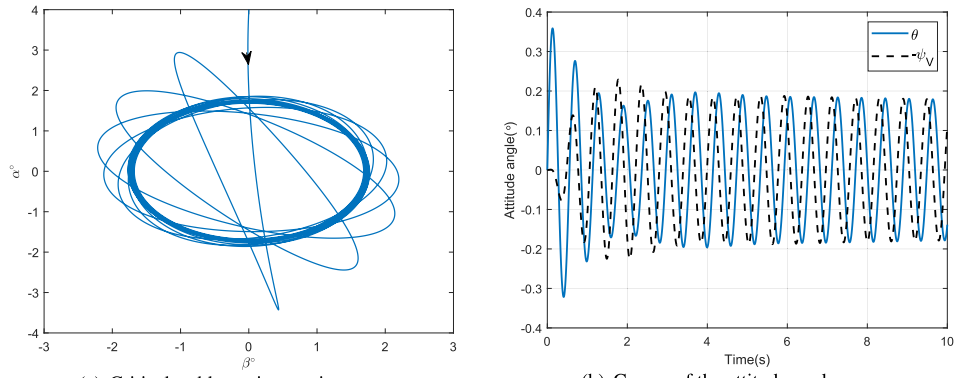

(a) Critical stable coning motion (b) Curves of the attitude angle

FIGURE 9. Response curves with design parameters on the stable boundary ($K_Z = 12.5, k_\omega = 0.086$).

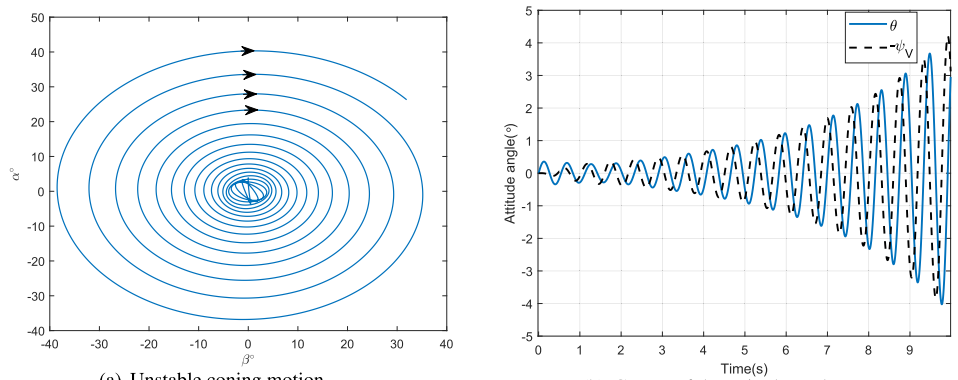

(a) Unstable coning motion (b) Curves of the attitude angle

FIGURE 10. Response curves with design parameters beyond the stable region ($K_Z = 12.5, k_\omega = 0.08$).

In addition, $k_\omega = 0.15$ and $k_\omega = 0.08$ are selected for the stable cases and unstable cases, respectively. Numerical simulations are conducted with an initial angle of attack error $\alpha_0 = 4°$. The simulation results are shown in Fig. 8, Fig. 9 and Fig. 10.

The simulation results illustrated in Fig. 8 are simulated at $k_\omega = 0.15$. According to the simulation results, in the stable case, the influence of the initial disturbance acting on the autopilot can be eliminated. Fig. 9 presents the simulation results at $k_\omega = 0.086$, which is a gain located in the stability boundary. The motion of the airframe enters a limit-cycle state and never converges to the zero point. Fig. 10 shows the simulation results at $k_\omega = 0.08$, which is an unstable gain of the rolling missile, and the motion of the airframe diverges gradually. Consequently, the simulation results demonstrate that the stability conditions we achieve

for the velocity orientation autopilot can correctly reflect the stability of the designed autopilot.

IV. METHODS TO IMPROVE STABILITY

From this discussion, it can be seen that the rolling of a missile has a significant influence on the stability of the velocity orientation autopilot. With rolling of the airframe, the Magnus effect and gyroscopic effect occur. Additionally, the steady-state gain of the actuator decreases, and the control response direction of the actuator deviates from expectation. As a result, the stability and accuracy of the autopilot is highly degraded. Hence, some feasible measures for suppressing the impacts of rolling are presented.

A. ACTUATOR DYNAMICS

As an airframe rolls, the distinct changes in the expressions of the stability conditions are represented by the appearance of the parameters associated with the Magnus effect, gyroscopic effect and actuator dynamics.

The Magnus effect and gyroscopic effect are mainly related to the aerodynamic shape and rolling rate. The shape of the missile is already determined before the control system design, so it is more feasible to adjust the rolling rate to change the magnitudes of these effects. The rolling rate is usually a trade-off under many constraints. Many articles have explored this problem, and thus, it is not included in this paper.

For actuator dynamics, as previously stated, the rolling of the missile decreases the dynamic gain of the actuator and leads to a deviation in the control responses. These changes decrease the stability and accuracy of the autopilot.

As stated in Section II, the equivalent dynamic gain of the actuator is expressed as

$$k_r = \frac{1}{\sqrt{\left(1 - T_s^2\omega^2\right)^2 + (2\mu_s T_s\omega)^2}} \tag{38}$$

From the expression, it can be seen that $k_r \leq 1$ decreases with an increase in the rolling rate and the time constant of the actuator T_s. The steady-state deviation angleγ_c is expressed as

$$\gamma_c = \arccos \frac{1 - T_s^2\omega^2}{\sqrt{\left(1 - T_s^2\omega^2\right)^2 + (2\mu_s T_s\omega)^2}} \tag{39}$$

From the expression, it can be seen that the deviation angle increases with an increase in the rolling rate and actuator time constant.

In Fig. 11, the curves of the steady-state deviation angle that vary with the rolling rate are plotted with the determined actuator parameters. It is shown that with an increase in the rolling rate, the total delay angle increases. It is obvious that the time constant of the actuator has the same impacts on the deviation angle. As the total deviation angle $\gamma_d = \gamma_c + \tau\omega$, the total deviation angle is proportional to the command transmission delay τ.

Referring to the stability conditions, a large dynamic gain and small total deviation angle are needed to improve stability and accuracy. Based on this analysis, actuators with a small command transmission delay and small time constant are reasonable choices for increasing stability.

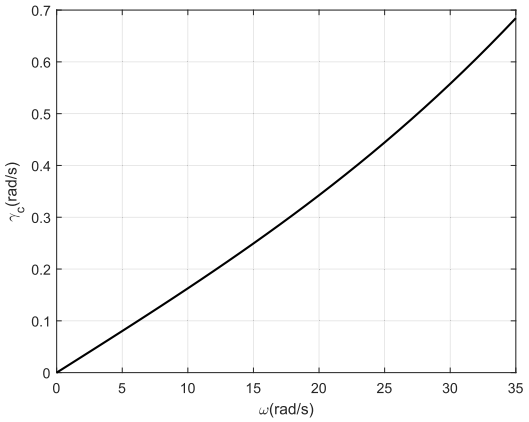

FIGURE 11. Steady-state deviation angle up to 35 with the rolling rate.

B. STATIC STABILITY

Static stability describes the capability of a missile to restore balance from a disturbance in the absence of control. It is a very important characteristic that is associated with the stability of missiles and is included in the static moment coefficient a_L. For static stable missiles and static unstable missiles, $a_L > 0$ and $a_L < 0$, respectively. The absolute value of a_L shows the degree of static stability. From Section II, the expression of the static moment coefficient is described as

$$a_L = -m_z^\alpha \frac{qS_{ref}l}{J_z} \tag{40}$$

where m_z^α is the derivative of the static moment coefficient, which is related to the positions of the mass center and pressure center and lift. Through the adjustment of the relative positions of the mass center and pressure center, the coefficient can be changed.

To demonstrate the influence of the static moment coefficient on the stability of rolling missiles, numerical simulations based on the stability conditions in Eq. (32) are conducted with rolling rate conditions of $\omega = 8\pi\ rad/s$ and derivatives of the static moment coefficient equal to -0.6589, -1.3178, and -1.9767. From Fig. 12, it can be seen that the stable region expands as the static moment coefficient increases, which means that we can increase the rolling missile stability by increasing the static stability of the missile. Additionally, as the value of the static moment coefficient increases linearly, the increase in the stability decreases gradually, which means that the efficiency of the stability improvement approach of increasing the static stability declines. In practice, static stability is also related to the maneuverability of the missile, and a large static stability means that the maneuverability of the missile decreases. As a result, a large but proper static stability should be chosen

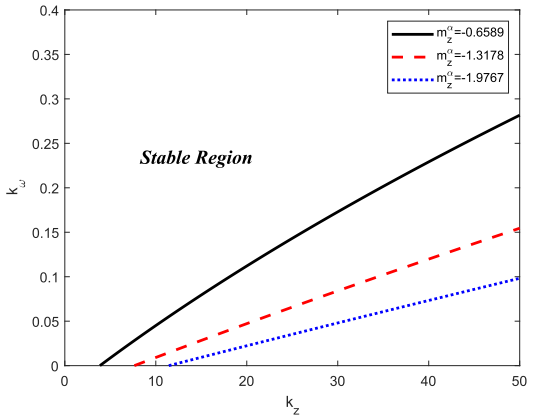

FIGURE 12. Stable region with different derivatives of the static moment coefficient.

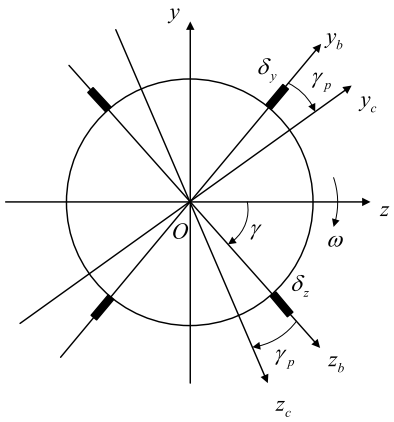

FIGURE 13. Schematic of leading angle.

with consideration of the stability and maneuverability in the design of missiles.

C. DECOUPLING

From this discussion, it is found that the total deviation angle affects the stability and accuracy of the velocity orientation autopilot. With determination of the autopilot parameters, the total deviation angle can be obtained with a certain accuracy. Thus, the decoupling method, which rotates a leading angle for actuator commands, can be used to improve stability.

Let the rotating angle be γ_p. With the decoupling method, the expression of the command resolution can be described as

$$\begin{bmatrix} \delta_z \\ \delta_y \end{bmatrix} = k_s k_r \begin{bmatrix} \cos\gamma_p & -\sin\gamma_p \\ \sin\gamma_p & \cos\gamma_p \end{bmatrix} \begin{bmatrix} \cos\gamma_d & \sin\gamma_d \\ -\sin\gamma_d & \cos\gamma_d \end{bmatrix} \begin{bmatrix} \delta_{zc} \\ \delta_{yc} \end{bmatrix} \tag{41}$$

This can be rewritten as

$$\begin{bmatrix} \delta_z \\ \delta_y \end{bmatrix} = k_s k_r \begin{bmatrix} \cos(\gamma_d - \gamma_p) & \sin(\gamma_d - \gamma_p) \\ -\sin(\gamma_d - \gamma_p) & \cos(\gamma_d - \gamma_p) \end{bmatrix} \begin{bmatrix} \delta_{zc} \\ \delta_{yc} \end{bmatrix} \tag{42}$$

Comparing equation (42) with (10), the new command resolution angle is equal to $\gamma_d - \gamma_p$. For a missile with a constant rolling rate, the leading angle can be chosen to be equal to the total deviation angle so that the new command resolution angle equals zero. Therefore, the control cross-couplings caused by the total deviation angle are completely decoupled. The leading angle is illustrated in Fig. 13.

The proposed decoupling methods for the cross-coupling of a servo system is validated in Fig. 14. Fig. 14 shows the step responses of actuators, and Fig. 15 shows the sine responses of actuators. According to the results, we found that the proposed lead angle decoupling method can effectively offset the coupling component, while the pitch channel is

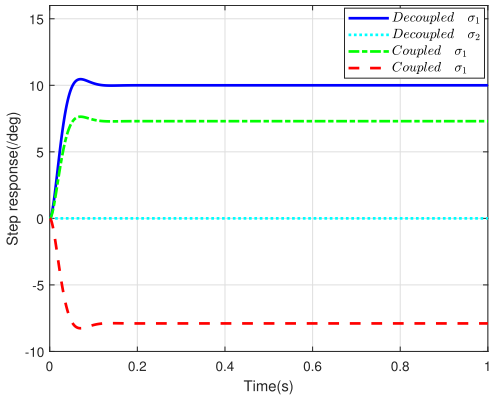

FIGURE 14. Step response of actuator.

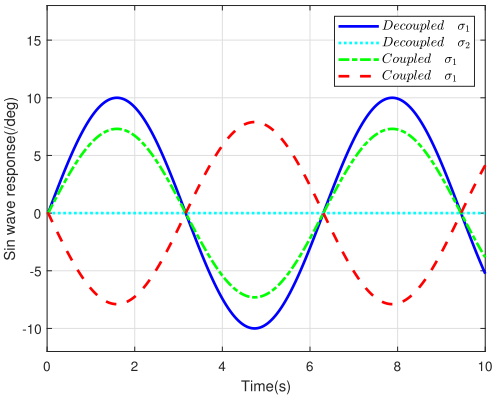

FIGURE 15. Sine wave response of actuator.

given a step signal or sine signal. Considering the missile aerodynamic model presented in Eq. (5), Fig. 16 and Fig. 17 explain the correctness of the coupled six degrees-of-freedom mathematical model.

To illustrate the robustness of the velocity orientation autopilot of a rolling missile, the Monte Carlo simulation is conducted with consideration for the deviation rolling rate and uncertain aerodynamic parameters of a missile [22], [24].

TABLE 2. Comparisons between the critical design parameters of cases with and without decoupling.

k_ω	$\omega = 6\pi$rad/s		$\omega = 8\pi$rad/s		$\omega = 10\pi$rad/s		$\omega = 12\pi$rad/s	
	without	with	without	with	without	with	without	with
0.05	9.6322	10.3867	9.4669	10.3218	9.2207	10.2562	7.4989	10.1678
0.10	15.4257	17.8077	14.5517	17.7290	13.3572	17.6484	10.3535	17.5495
0.15	21.8076	25.7918	20.2730	25.6844	18.2265	25.5733	14.0574	25.4511
0.20	28.7805	34.3392	26.6365	34.1883	23.8446	34.0310	18.6966	33.8730
0.25	36.3470	43.4498	33.6473	43.1510	30.2256	43.0218	24.3409	42.8154
0.30	44.5090	53.1239	41.3099	52.8419	37.3818	52.5459	31.0489	52.2784
0.35	53.2688	63.3616	49.6287	62.9919	45.3242	62.6034	38.8693	62.2624

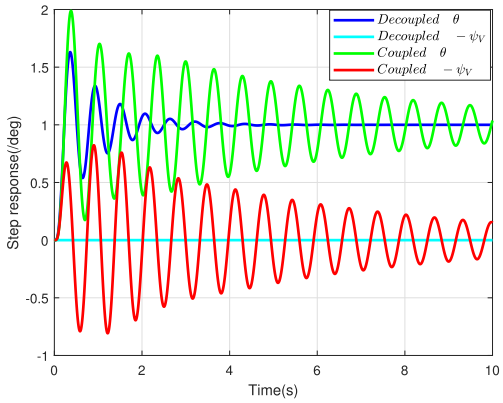

FIGURE 16. Step response of missile.

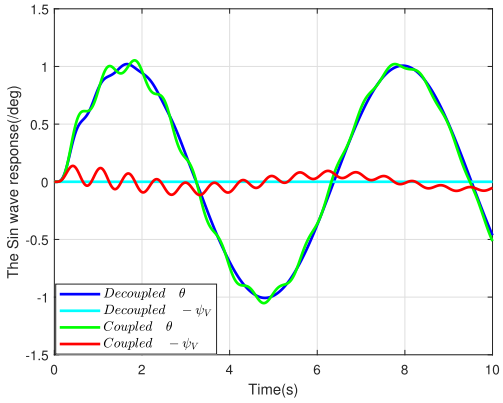

FIGURE 17. Sine wave response of missile.

The result is shown in Fig. 18. We determined that the system can be kept steady under the effect of interference.

To further verify the effectiveness of the decoupling method, numerical simulations at different rolling rates are conducted based on the stability conditions in Eq. (32). The parameters of the rolling missile are the same as those listed in TABLE 1. The critical design parameters of the velocity orientation autopilot with and without the decoupling method are shown in TABLE 2. TABLE 2 shows that with the decoupling method applied, the stable region of the autopilot design parameters extends considerably. Moreover, it is shown that the stability improves as the gain of the inner loop increases and worsens as the rolling rate increases, which matches the analysis results. In practical applications, the leading angle is

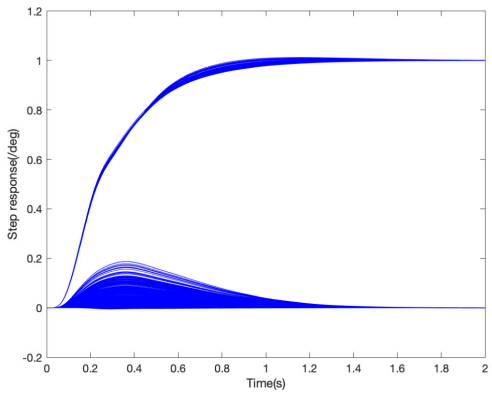

FIGURE 18. Monte Carlo simulation.

usually achieved by installing sensors with advanced installation angles along the rolling direction. However, due to the absence of roll control autopilot, the rolling rate of the missile often varies due to disturbances from the environment during flight, so the total deviation angle changes. In this case, a rate gyro can be applied to measure the real-time rolling rate and then compensate for the decoupling. The decoupling method is effective and easy to apply to improve the dynamic stability.

V. CONCLUSION

In this paper, the sufficient and necessary stability conditions for rolling missiles with velocity orientation autopilot are obtained by mathematical derivation. Numerical simulations are conducted to verify the accuracy of the conditions. The analysis of the stability conditions indicates that the total deviation angle of the control system should not exceed 90°. If the total deviation angle of the control system exceeds 90°, the gain of the rate feedback is seriously limited, which makes it difficult to obtain the desired velocity orientation autopilot. A comparison between the stability conditions of rolling missiles and those of nonrolling missiles shows that the stability of the velocity orientation autopilot is degraded due to rolling of the airframe. The achieved stability conditions can reflect the effect of rolling on stability. Based on this discussion, some approaches are introduced to improve stability. Considering the reduction in stability induced by the actuator dynamics, actuators with small time constants (fast response speeds) and short command transmission times should be employed for rolling missiles. Static stability is

a very important factor related to stability and the control system design. Increasing static stability can greatly improve stability. Considering the control cross-coupling induced by the total deviation angle, a decoupling method that rotates the leading angle for actuator commands can be applied to increase stability. With numerical simulation, the effectiveness of these approaches is demonstrated. In conclusion, the stability analysis method and the achieved stability conditions have instructive significance to the engineering design of the velocity orientation autopilot of rolling missiles. In this paper,we only consider the dynamic stability of the velocity orientation autopilot that designed through classical control theory, for further studies,the dnamic stability of the autopilot in rolling frame taht designed through modern control theories such as sliding mode control and LQR control theory can be taken into consider. Moreover,this paper only proposed a simple decoupling method of setting a lead angle to compensate control coupling,therrfore many advance decoupling methods like inverse dynamic theory and neural network can invetigate to eliminate coupling.

REFERENCES

[1] P. Koprinkova and V. Penev, "Dynamical behavior of fuzzy logic based velocity control autopilot with respect to changes in linguistic variables membership functions shape," *Inf. Secur., Int. J.*, vol. 3, pp. 108–115, Jan. 1999.
[2] Z. Qi and D. Lin, *Design of Guidance and Control Systems for Tactical Missiles*. Boca Raton, FL, USA: CRC Press, 2019.
[3] J.-M. Song, "Research on attitude pursuit guidance law for strapdown homing system," *Chin. J. Aeronaut.*, vol. 17, no. 4, pp. 235–239, Nov. 2004.
[4] H. L. Pastrick, S. M. Seltzer, and M. E. Warren, "Guidance laws for short-range tactical missiles," *J. Guid. Control*, vol. 4, no. 2, pp. 98–108, Mar. 1981.
[5] P. Garnell, D. J. East, and G. M. Siouris, "Guided weapon control systems," *IEEE Trans. Syst., Man, and*, vol. I-9, no. 11, pp. 740–741, Nov. 1979.
[6] P. Zarchan, "Tactical and strategic missile guidance," Amer. Inst. Aeronaut. & Astronaut., Reston, VA, USA, Tech. Rep., Jan. 1990, vol. 176.
[7] G. M. Siouris, *Missile Guidance and Control Systems*. New York, NY, USA: Springer, 2004.
[8] X. Mao, S. Yang, and Y. Xu, "Coning motion stability of wrap around fin rockets," *Sci. China E: Technol. Sci.*, vol. 50, no. 3, pp. 343–350, Jun. 2007.
[9] G. Liaño and J. Morote, "Roll-rate stability limits of unguided rockets with wraparound fins," *J. Spacecraft Rockets*, vol. 43, no. 4, pp. 757–761, Jul. 2006.
[10] J. Morote and G. Liano, "Flight dynamics of unguided rockets with free-rolling wrap around tail fins," *J. Spacecraft Rockets*, vol. 43, no. 6, pp. 1422–1423, Nov. 2006.
[11] C. Mracek, M. Stafford, and M. Unger, "Control of spinning symmetric airframes," Nat. Tech. Inf. Service, Springfield, VA, USA, Rep. 24, Nov. 2006.
[12] D. H. Platus, "Ballistic re-entry vehicle flight dynamics," *J. Guid., Control, Dyn.*, vol. 5, no. 1, pp. 4–16, Jan. 1982.
[13] D. H. Platus, "Missile and spacecraft coning instabilities," *J. Guid., Control, Dyn.*, vol. 17, no. 5, pp. 1011–1018, Sep. 1994.
[14] C. H. Murphy, "Angular motion of a re-entering symmetric missile," *AIAA J.*, vol. 3, no. 7, pp. 1275–1282, Jul. 1965.
[15] C. Murphy, "Free flight motion of symmetric missiles," Ballistic Res. Lab., Aberdeen Proving Ground, MD, USA, Rep. 241, Jul. 1963.
[16] C. H. Murphy, "Symmetric missile dynamic instabilities," *J. Guid. Control*, vol. 4, no. 5, pp. 464–471, Sep. 1981.
[17] P. W. Fortescue and E. M. Belo, "Control decoupling analysis for gyroscopic effects in rolling missiles," *J. Guid., Control, Dyn.*, vol. 12, no. 6, pp. 798–805, Nov. 1989.
[18] X. Yan, S. Yang, and C. Zhang, "Coning motion of spinning missiles induced by the rate loop," *J. Guid., Control, Dyn.*, vol. 33, no. 5, pp. 1490–1499, Sep. 2010.
[19] X. Yan, S. Yang, and F. Xiong, "Stability limits of spinning missiles with attitude autopilot," *J. Guid., Control, Dyn.*, vol. 34, no. 1, pp. 278–283, Jan. 2011.
[20] K. Li, S. Yang, and L. Zhao, "Stability of spinning missiles with an acceleration autopilot," *J. Guid., Control, Dyn.*, vol. 35, no. 3, pp. 774–786, May 2012.
[21] S. Yang, L. Zhao, and X. Yan, *Dynamic Stability of Spinning Missiles*. Beijing, China: National Defense Industry Press, 2014.
[22] M. R. Mohammadi, M. F. Jegarkandi, and A. Moarrefianpour, "Robust roll autopilot design to reduce couplings of a tactical missile," *Aerosp. Sci. Technol.*, vol. 51, pp. 142–150, Apr. 2016.
[23] E. Frank, "On the zeros of polynomials with complex coefficients," *Bull. Amer. Math. Soc.*, vol. 52, pp. 144–157, Jan. 1946.
[24] P. K. Trivedi, B. Bandyopadhyay, S. Mahata, and S. Chaudhuri, "Roll stabilization: A higher-order sliding-mode approach," *IEEE Trans. Aerosp. Electron. Syst.*, vol. 51, no. 3, pp. 2489–2496, Jul. 2015.

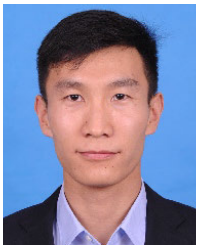

SHAOYONG HU was born in Henan, China. He received the B.Eng. degree in mechanical design manufacturing and automation from Central South University, in 2014. He is currently pursuing the Ph.D. degree with the School of Aerospace Engineering, Beijing Institute of Technology, Beijing, China. His research interests include missile guidance and control, inertial navigation, and integrated navigation.

JIANG WANG received the Ph.D. degree in flying vehicle design from Beijing Institute of Technology, in 2008. He is currently a Professor with the School of Aerospace Engineering, Beijing Institute of Technology. His research interests include missile guidance and control and UAV formation control.

YUCHEN WANG was born in Xi'an, Shaanxi, China. He received the B.Eng. degree in mechanical engineering from Ningxia University, in 2018. He is currently pursuing the Ph.D. degree with the School of Aerospace Engineering, Beijing Institute of Technology, Beijing, China. His research interests include flight vehicle guidance and control and advanced control theory.

SONG TIAN received the Ph.D. degree in flying vehicle design from Beijing Institute of Technology, in 2020. He is currently working with Beijing System Design Institute of Electro-Mechanic Engineering. His research interests include missile guidance and control.